Mitigation of Dispersion and Turbulence in a Hybrid Optical Fibre and Free-Space Optics Link Using Electronic Equalisation

Dong-Nhat NGUYEN [a,1], Stanislav ZVANOVEC [a,2], Zabih GHASSEMLOOY [b,3]

[a] Dept. of Electromagnetic Field, Czech Technical University in Prague, Technicka 2, 166 27 Prague, Czech Republic
[b] Optical Communication Research Group, Faculty of Engineering and Environment, Northumbria University, Newcastle upon Tyne, NE1 8ST, United Kingdom

[1]dongnhat@fel.cvut.cz; [2]xzvanove@fel.cvut.cz; [3]z.ghassemlooy@northumbria.ac.uk

Abstract

Transmission of a 25 Gbps non-return to zero signal over a hybrid link of 20 km standard single-mode fibre and 500 m free-space optics under weak-to-moderate turbulence regimes is demonstrated via simulation to provide a practical solution for the last-mile access networks. Even though there are several complex mitigating methods to reduce the waveform distortions caused by both the fibre chromatic dispersion and atmospheric turbulence, we provide and discuss a simple approach using an electrical equalizer at the receiver. The simulation results demonstrate that, the proposed equalization technique offer about an order of magnitude improvement in the bit error rate at the received optical power of -20 dBm and a receiver sensitivity gain of 1.5 dB at the 7% forward error correction limit.

Keywords: Optical access networks, chromatic dispersion, free-space optics, electronic equalization, atmospheric turbulence

1. Introduction

Enterprise connectivity and last-mile access networks present challenges for the service providers in delivering high-speed data networks to the end users. Unlicensed and licensed radio frequency (RF) wireless technologies can be adopted but with several constraints (e.g., limited bandwidth, low data rate and high interference susceptibility) [1]. Free space optical (FSO) communications have recently attracted significant attention due to several advantages such as a wide unlicensed frequency spectrum, inherent security and immunity to RF induced electromagnetic interference and lower power consumption [2–4]. Moreover FSO system can be rapidly deployed when fibre is unpractical to install due to the geographical restrictions or physical obstacles. FSO systems are therefore suitable to implement as an extension of an optical access network and the last mile access. Such systems are also used in hybrid radio over free-space optical (RoFSO) or in all-optical hybrid optical fibre (OF) and FSO (OF-FSO) communication systems [5–9]. Considering their narrow beam widths (i.e., high level of security at the physical layer) and a very large license-free frequency band, as compared with microwave systems, FSO links are suitable candidates for secure, high-speed, cost-effective and wide-bandwidth communications.

In [10], indoor experimental demonstrations of hybrid OF-FSO transmission links were reported with the focus on the impact of the atmospheric turbulence. It was shown that, under high-levels of turbulence the propagating optical beams experienced both intensity and phase fluctuations, which resulted in both changes optical illumination area (i.e., optical footprint) and beam wondering at the receiver (Rx) and thus consequently deteriorating the signal quality.

A number of turbulence mitigation techniques such as spatial transmitter (Tx)/Rx diversity, adaptive beamforming, multiple-beam communication or novel modulation techniques [1,11] have been proposed but at the cost of increased circuit complexity and signal processing requirements. To date, only a few studies have been reported on the fully integrated OF and a long length outdoor FSO links [3,12]. In [3], a 20 channels ultra-

dense wavelength-division multiplexed passive optical network at 625 Mbaud over 100 km standard single-mode fibre (SMF) and 54 m long FSO links was successfully demonstrated using dual-polarization quadrature phase-shift keying (DP-QPSK) modulation and a coherent Rx. In [12], 18 Gbaud 32-quadrature amplitude modulation (32-QAM) transmission using an in-phase and quadrature modulator and a tunable optical filter was demonstrated over 22 km of SMF and 100 m FSO links. However, in [3,12] the modulation formats, devices and the detection method adopted were too complex and costly for the practically low-cost optical access networks [13–15]. In [16], a bidirectional 10 Gbps hybrid OF-FSO link for use in outdoor environments was proposed, where an erbium-doped fibre amplifier was employed to compensate for losses due to the OF-FSO channel.

Following hybrid OF-FSO transmission, the waveform experience both dispersion and turbulence induced dispersion, which can be mitigated at the Rx by using an adaptive electrical equalizer (EEQ). It is worth noting that, EEQ has been demonstrated mostly to mitigate only fibre transmission impairments such as modal, chromatic and polarization-mode dispersions [17,18]. Two well-known and low-complexity electronic equalization technologies have been widely employed – feed-forward equalizer (FFE) and decision-feedback equalizer (DFE). More details on FFE and DFE for direct detection-based systems can be found in [19]. In this paper, we report for the first time, a 25 Gbps hybrid OF-FSO link for the last-mile access network utilizing a simple EEQ at the Rx to compensate for the aggregate effect of chromatic dispersion-induced intersymbol interference and turbulence-induced fading.

The remaining of the paper is organized as follows: Section 2 briefly presents the principle of FSO link under atmospheric turbulence. Section 3 explains the simulation setup while the results are presented and discussed in Section 4. Finally, Section 5 concludes the findings of the paper.

2. Atmospheric Turbulence Model

Turbulence-induced fading is the main factor that degrades the performance of FSO links. This is due to the variations of the refractive index along the transmission path initiated by inhomogeneities in the temperature and pressure of the atmosphere [20]. These inhomogeneities can severely deteriorate the signal quality and therefore increase the errors in the received signal. Two distribution models have been widely used to statistically describe the turbulence-induced fading are Log-normal and Gamma-Gamma (GG) [10,20]. The GG model is used in the present study and its probability density function is expressed by [20]

$$f_{GG}(h_s) = \frac{2(\alpha\beta)^{(\alpha+\beta)/2}}{\Gamma(\alpha)\Gamma(\beta)} (h_s)^{((\alpha+\beta)/2)-1} \times K_{\alpha-\beta}\left(2\sqrt{\alpha\beta h_s}\right) \tag{1}$$

where $\Gamma(\cdot)$ denotes the Gamma function and $K_{\alpha-\beta}(\cdot)$ is the modified Bessel function of the second kind of order $(\alpha - \beta)$. The parameters α and β are the effective number of large-scale and small-scale eddies of the scattering process, respectively. For plane wave propagation the parameters are given by [9]

$$\alpha = \left[exp\left(\frac{0.49\sigma_R^2}{\left(1+1.11\sigma_R^{12/5}\right)^{7/6}} \right) - 1 \right]^{-1} \tag{2}$$

$$\beta = \left[exp\left(\frac{0.51\sigma_R^2}{\left(1+0.69\sigma_R^{12/5}\right)^{5/6}} \right) - 1 \right]^{-1} \tag{3}$$

where σ_R^2 is Rytov variance used to describe the atmospheric turbulence strengths, which can be expressed as [9]

$$\sigma_R^2 = 1.23 C_n^2 \left(\frac{2\pi}{\lambda}\right)^{7/6} L_{FSO}^{11/6} \tag{4}$$

where

$$C_n^2 = \left(79 \times 10^{-6} \frac{P}{T^2}\right)^2 C_T^2 \quad (5)$$

C_n^2 $(m^{-2/3})$ represents the refractive index structure parameter (the most important parameter to describe the turbulence strength), P is the atmospheric pressure in millibar, T stands for the average temperature in Kelvin and C_T^2 is the temperature structure constant, which is defined as [20]

$$C_T^2 = (T_1 - T_2)^2 / L^{2/3} \quad (6)$$

where T_1 and T_2 are temperatures at two points separated by distance L. Having known the thermal profiles along the FSO transmission path C_n^2 can then be determined.

3. Simulation Setup

Fig. 1(a) presents the system block diagram of the deployment of hybrid OF-FSO for the last-mile application in the optical access network. Fig. 1(b) illustrates the simulation setup of the proposed hybrid OF-FSO system including Rx-based equalization to compensate for the joint distortion due to the OF dispersion and FSO atmospheric turbulence. A 25 Gbps non-return to zero (NRZ) signal is used for external modulation of the continuous-wave laser output with the power of 3 dBm at 1550 nm using a $LiNbO_3$ Mach-Zehnder modulator (MZM). The switching bias voltage of MZM was set to 4 V and its output signal (at 0 dBm) was launched into a 20 km OF, which is the standard SMF link with a dispersion parameter of 17 ps/nm/km representing the fibre-based backbone part. Note that, details of the optical fibre model adopted in this work can be found in [21]. We then have used a FSO transmitter to launch the light beam to the free-space of a 500 m link span, which represents a typical distance in urban areas for access networks. Note that, both FSO transceivers used have an aperture diameter of 2.54 cm, in order to be consistent with our experimental FSO links [10,22]. We investigate the link performance with the FSO channel set with clear (i.e., attenuation of 0.2 dB/km) and weak-to-moderate turbulence conditions.

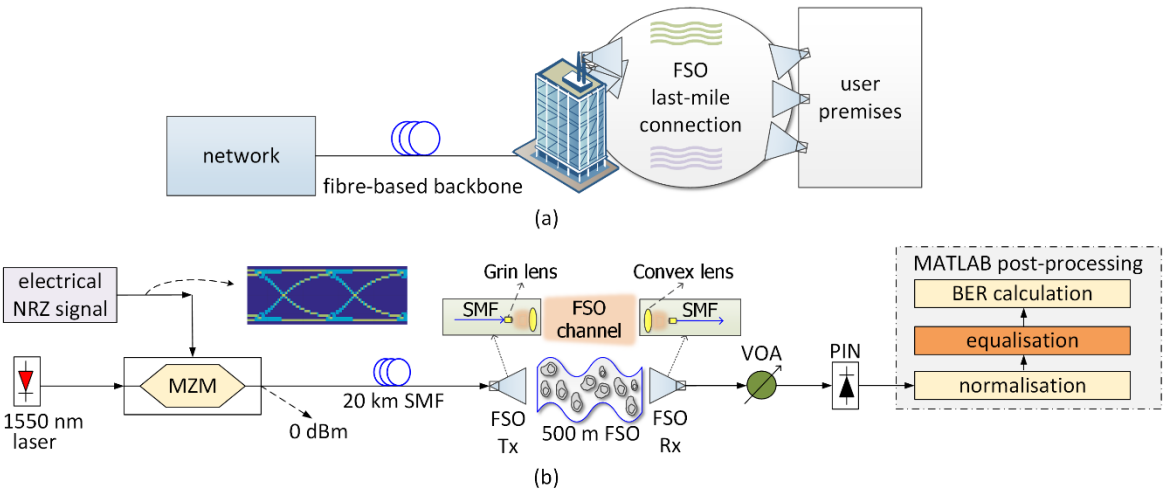

Fig. 1. A Hybrid OF-FSO network: (a) concept and (b) simulation setup

At the Rx, a variable optical attenuator (VOA) is used to adjust the received optical power P_r, followed by a PIN photodetector. The electrical signal is captured and then post-processed using MATLAB (i.e., normalization and equalisation) prior to determine link's bit error rate (BER) performance. To compensate for the dispersion and turbulence-induced waveform distortions FFE and DFE were selected since they do not introduce additional losses and have lower power consumptions. The coefficients for the equalisers are determined using the normalised least-mean square (LMS) algorithm. Note that, for equalisers we have adopted a symbol-spaced mode and a fixed step-size μ of 0.0015. The proposed system is simplified by using NRZ

based intensity modulation and direct detection transmission link with no optical amplifiers, optical filters and dispersion compensation modules. All the key system parameters adopted are summarized in Table 1.

Table 1. Main parameters used in simulation

Parameter	Value
Data format	NRZ
Data rate	25 Gbps
Pseudo-random binary sequence	2^{15}-1
Wavelength	1550 nm
Optical transmit power	0 dBm
OF length	20 km
Fibre dispersion	17 ps/nm/km
FSO length	500 m
Turbulence strength	10^{-16}, 10^{-14} $m^{-2/3}$
Lens aperture diameter	2.54 cm
FFE taps	0-71
DFE taps	0-7

4. Simulation Results

4.1 Back-to-Back Link

First, we investigate the system performance for the back-to-back (B2B) link (i.e., no hybrid OF-FSO channel included) by means of simulation using OptiSystem software. Figure 2 depicts BER performance of a NRZ B2B link with no equalisers for a range of data rates of 10, 25 and 50 Gbps. Note that, 25 and 50 Gbps have already been adopted by the IEEE P802.3ca Task Force as part of the future upgrades of current 10G optical access networks [15]. Also shown in Fig. 2 is the 7% overhead hard decision forward error correction (FEC) BER limit of 3.8×10^{-3}. At the FEC limit, the optical power penalties are 2 and 3.6 dB for 25 and 50 Gbps, respectively compared with the 10 Gbps link. The results agree very well with the experimental data reported in [15], thus verifying the proposed simulation set-up. The inset in Fig. 2 shows a clear eye opening observed for the 25 Gbps B2B link.

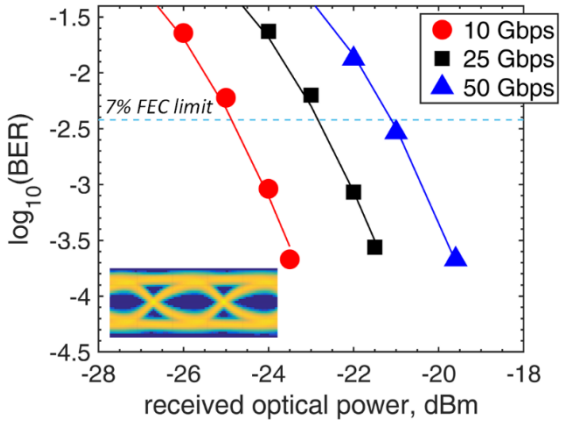

Fig. 2. BER performance for the B2B link at 10, 25 and 50 Gbps. The inset shows the received eye diagram for 25 Gbps

4.2 Hybrid Optical Link

Next, we investigate the link with FFE and DFE. Figs. 3 (a) and (b) depict the BER as a function of the number of taps for FFE and DFE for weak (i.e., $C_n^2 = 1 \times 10^{-16}\, m^{-2/3}$) and moderate (i.e., $C_n^2 = 1 \times 10^{-14}\, m^{-2/3}$) turbulence regimes, respectively at P_r of -20 dBm for 20 km and 500 m of OF and FSO links.

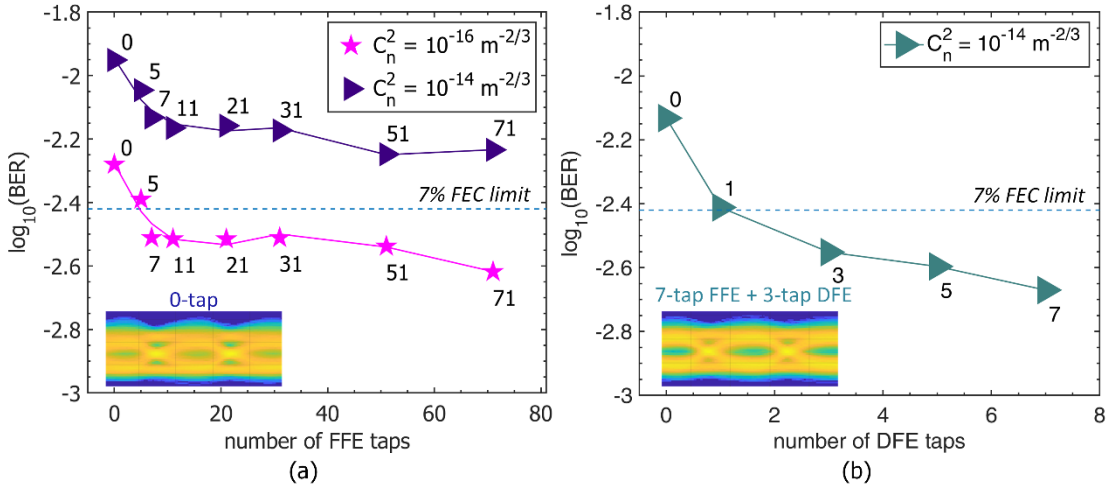

Fig. 3. BER versus FFE and DFE taps for 25 Gbps NRZ at P_r of -20 dBm in the hybrid link of 20 km OF and 500 m FSO with: (a) weak and moderate turbulences with FFE implemented and (b) moderate turbulence with 7-tap FFE and increased taps DFE implemented. Insets demonstrate the eye diagrams for particular taps

As can be seen from the Fig. 3(a), with no EEQ, the BER is high well above the 7% FEC limit, which is attributed to the fibre chromatic dispersion and atmospheric turbulence-induced distortion (see the inset eye diagram). The link performance is enhanced by using EEQs, where lower BERs are achieved for a higher number of taps (i.e. 71-tap FFE). For hybrid transmisison under weak turbulence, the BER is lower than the FEC limit for FFE with > 6 taps. Increasing the num ber of taps beyond 7 results in marginal improvement in the BER performance. However, for hybrid transmission with moderate turbulence at the same P_r of -20 dBm the BER plot is well above the FEC limit, thus illustrating unsuitability of FFE mitigate the distortions. In order to improve the BER, which is degraded by the aggregate impairments, we have used a combination of both FFE and DFE. See the results illustrated in Fig. 3(b) and also shown the inset eye diagram, where the BER improves with higher number of DFE taps. As shown, with only 7-tap FFE and 2-tap DFE the BER is below the 7% FEC limit.

Following optimization of the EEQ module, which consists of 7-tap FFE and 3-tap DFE also denoted as EEQ(7,3), we investigate the BER performance under weak-to-moderate turbulence regime (i.e., C_n^2 of 1×10^{-16}, 1×10^{-15} and $1 \times 10^{-14}\, m^{-2/3}$) and for 25 Gbps NRZ at P_r of -20 dBm for the hybrid link of 20 km and 500 m of OF and FSO, respectively as shown in Fig. 4. Note, the link with EEQ(7,3) offers improved performance in comparison to the link with no EEQ, which adaptively compensates for dispersion and turbulence, and is below the 7% FEC limit. However, the BER improvement margin is less at higher turbulence levels. Therefore, at higher turbulence levels (i.e., $< 1 \times 10^{-14}\, m^{-2/3}$) a combination of FFE and DFE with higher number of taps and advanced digital signal processing techniques should be adopted.

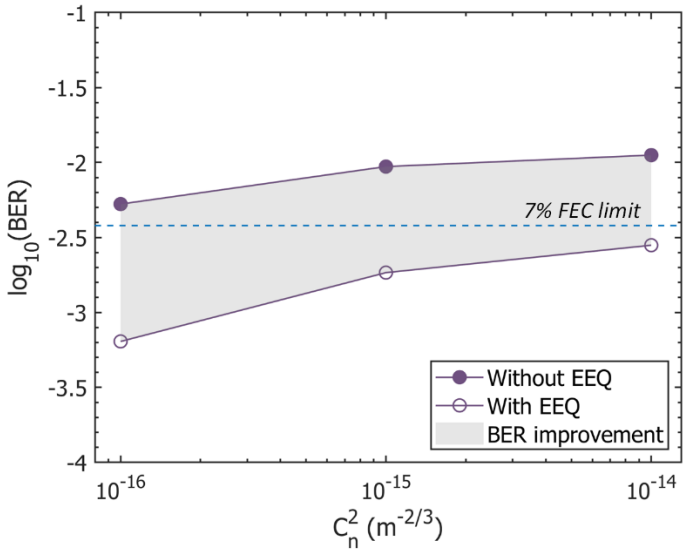

Fig. 4. BER versus the atmospheric turbulence for 25 Gbps NRZ at P_r of -20 dBm in the hybrid link of 20 km OF and 500 m FSO without and with equalisation by 7-tap FFE and 3-tap DFE

Finally, to illustrate EEQ performance in separate parts, Fig. 5 (a) shows the BER performance against P_r for 25 Gbps NRZ without and with EEQ (7-tap FFE and 3-tap DFE) following transmission over a 20 km OF (i.e., without FSO channel), while Figs. 5 (b) and (c) display the results of a 20 km OF and an extended FSO link of 500 m long under weak and moderate turbulence conditions, respectively. With no EEQ, at the 7% FEC threshold level we observe ~ 2.8, 3 and 4 dB of optical power penalties for the 20 km OF link only, and the hybrid link under weak and moderate turbulence regimes, respectively compared to the B2B link. However, for all cases, the Rx sensitivity is enhanced by 1.5 dB at the 7% FEC limit and about one order of magnitude improvement in the BER performance at P_r of - 20 dBm.

From Fig. 5, we also observe that simple EEQ in general improves the overall performance of the hybrid link. However, regarding the aggregate impairments, EEQ shows a great enhancement in compensating the dispersion but less for turbulence. This can be explained that the turbulence effect is nondeterministic. Therefore, the FSO technology can be employed for last mile as part of hybrid OF-FSO-based access networks, given that the dispersion is well-compensated by the EEQ at the Rx. It is also worth mentioning that, in order to effectively mitigate the atmospheric turbulence at the Rx based on digital signal processing, an advanced technique should be considered i.e, 15-layer deep convolutional neural network [23], but at the cost of high complexity and implementation.

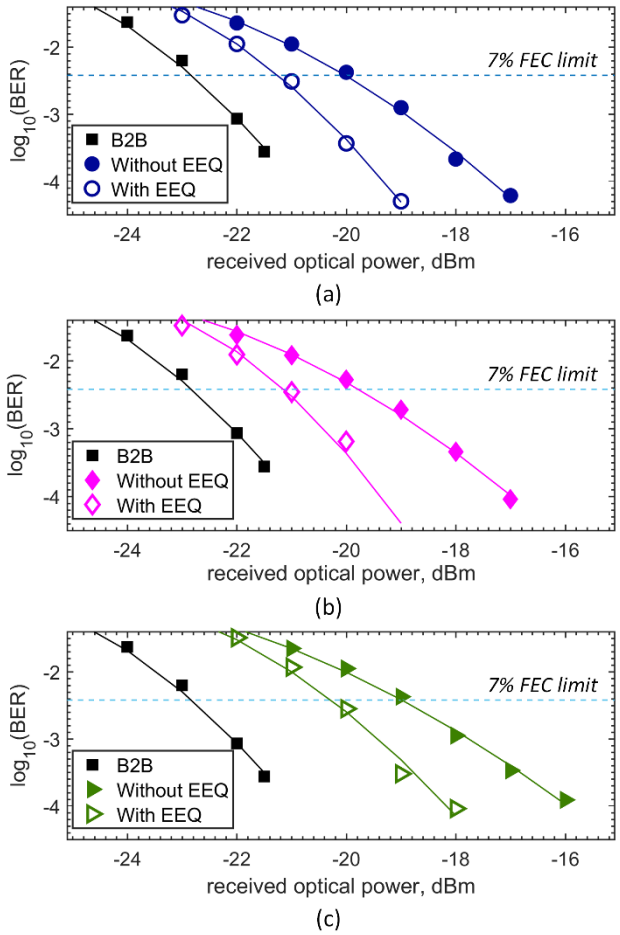

Fig. 5. BER performance at 25 Gbps without and with EEQ (7-tap FFE and 3-tap DFE) of different channel scenarios: (a) 20 km OF only, (b) 20 km OF and 500 m FSO with weak turbulence $C_n^2 = 10^{-16}\ m^{-2/3}$ and (c) 20 km OF and 500 m FSO with moderate turbulence $C_n^2 = 10^{-14}\ m^{-2/3}$

5. Conclusion

We have numerically demonstrated for the first time the utilization of adaptive electronic equalisation to compensate for the waveform distortions caused by the accumulated effect of chromatic dispersion and atmospheric turbulence in a hybrid optical link of 20 km of OF and 500 m of FSO. We showed that, the link performance under the cumulative effects can be improved by using FFE and become more efficient by adopting a combination of FFE and DFE. About an order of magnitude BER improvement was achieved by adopting the proposed technique, which could be adaptively set for a wide range of turbulence regimes. Our next step in this area will be focused on the experimental validation of the proposed method.

Acknowledgments

International mobility of researchers in CTU (CZ.02.2.69/0.0/0.0/16_027/0008465) and INTER-COST project (LTC18008) under the frame of COST CA16220.

References

1. M. A. Khalighi and M. Uysal, "Survey on free space optical communication: a communication theory perspective," IEEE Commun. Surv. Tutorials **16**(4), 2231–2258 (2014).

2. Z. Ghassemlooy, W. O. Popoola, and S. Rajbhandari, *Optical Wireless Communications – System and Channel Modelling with Matlab*, 2nd ed. (CRC Press, 2019).

3. A. N. Sousa, I. A. Alimi, R. M. Ferreira, A. Shahpari, M. Lima, P. P. Monteiro, and A. L. Teixeira, "Real-time dual-polarization transmission based on hybrid optical wireless communications," Opt. Fiber Technol. **40**, 114–117 (2018).

4. Z. Ghassemlooy, S. Arnon, M. Uysal, Z. Xu, and J. Cheng, "Emerging optical wireless communications-advances and challenges," IEEE J. Sel. Areas Commun. **33**(9), 1738–1749 (2015).

5. K. Kazaura, K. Wakamori, M. Matsumoto, T. Higashino, K. Tsukamoto, and S. Komaki, "RoFSO: A universal platform for convergence of fiber and free-space optical communication networks," IEEE Commun. Mag. **48**(2), 130–137 (2010).

6. J. Bohata, S. Zvanovec, T. Korinek, M. Abadi, and Z. Ghassemlooy, "Characterization of dual-polarization LTE radio over a free-space optical turbulence channel," Appl. Opt. **54**(23), 7082–7087 (2015).

7. J. Bohata, S. Zvánovec, P. Pešek, T. Kořínek, M. Abadi, and Z. Ghassemlooy, "Experimental verification of long-term evolution radio transmissions over dual-polarization combined fiber and free-space optics optical infrastructures," Appl. Opt. **55**(8), 2109–2116 (2016).

8. H. K. Al-Musawi, T. Cseh, J. Bohata, W. P. Ng, Z. Ghassemlooy, S. Zvanovec, E. Udvary, and P. Pesek, "Adaptation of mode filtering technique in 4G-LTE hybrid RoMMF-FSO for last-mile access network," J. Lightwave Technol. **35**(17), 3758–3764 (2017).

9. C. Ben Naila, K. Wakamori, M. Matsumoto, A. Bekkali, and K. Tsukamoto, "Transmission analysis of digital TV signals over a radio-on-FSO channel," IEEE Commun. Mag. **50**(8), 137–144 (2012).

10. N. A. M. Nor, Z. Ghassemlooy, J. Bohata, P. Saxena, M. Komanec, S. Zvanovec, M. R. Bhatnagar, and M.-A. Khalighi, "Experimental investigation of all-optical relay-assisted 10 Gb/s FSO link over the atmospheric turbulence channel," J. Lightwave Technol. **35**(1), 45–53 (2017).

11. H. Kaushal and G. Kaddoum, "Optical communication in space: challenges and mitigation techniques," IEEE Commun. Surv. Tutorials **19**(1), 57–96 (2017).

12. M. A. Esmail, A. Ragheb, H. Fathallah, and M.-S. Alouini, "Investigation and demonstration of high speed full-optical hybrid FSO/fiber communication system under light sand storm condition," IEEE Photonics J. **9**(1), 1–12 (2017).

13. D. T. Van Veen and V. E. Houtsma, "Proposals for cost-effectively upgrading passive optical networks to a 25G line rate," J. Lightwave Technol. **35**(6), 1180–1187 (2017).

14. N. Dong-Nhat, L. Nguyen, and A. Malekmohammadi, "Using duobinary with first- and second-order optical equalisers for extending transmission distance of optical access networks," IET Optoelectron. **12**(5), 239–243 (2018).

15. V. Houtsma, D. T. Van Veen, and H. Chow, "Demonstration of symmetrical 25 Gb/s TDM-PON with multilevel interleaving of users," J. Lightwave Technol. **34**(8), 2005–2010 (2016).

16. Y.-L. Yu, S.-K. Liaw, H.-H. Chou, H. Le-Minh, and Z. Ghassemlooy, "A hybrid optical fiber and FSO system for bidirectional communications used in bridges," IEEE Photonics J. **7**(6), 1–9 (2015).

17. J. M. Castro, R. Pimpinella, B. Kose, P. Huang, B. Lane, K. Szczerba, P. Westbergh, T. Lengyel, J. S. Gustavsson, A. Larsson, and P. A. Andrekson, "Investigation of 60 Gb/s 4-PAM Using an 850 nm VCSEL and Multimode Fiber," J. Lightwave Technol. **34**(16), 3825–3836 (2016).

18. H. F. Haunstein, W. Sauer-Greff, A. Dittrich, K. Sticht, and R. Urbansky, "Principles for electronic equalization of polarization-mode dispersion," J. Lightwave Technol. **22**(4), 1169–1182 (2004).

19. N. Eiselt, H. Griesser, J. Wei, R. Hohenleitner, A. Dochhan, M. Ortsiefer, M. H. Eiselt, C. Neumeyr, J. J. V. Olmos, and I. T. Monroy, "Experimental demonstration of 84 Gb/s PAM-4 over up to 1.6 km SSMF using a 20-GHz VCSEL at 1525 nm," J. Lightwave Technol. **35**(8), 1342–1349 (2017).

20. L. C. Andrews and R. L. Phillips, *Laser Beam Propagation through Random Media* (SPIE, 2005), **1**.

21. N. Dong-Nhat, M. A. Elsherif, and A. Malekmohammadi, "Investigations of high-speed optical transmission systems employing Absolute Added Correlative Coding (AACC)," Opt. Fiber Technol. **30**, 23–31 (2016).

22. J. Bohata, M. Komanec, J. Spáčil, Z. Ghassemlooy, S. Zvánovec, and R. Slavík, "24–26 GHz radio-over-fiber and free-space optics for fifth-generation systems," Opt. Lett. **43**(5), 1035–1038 (2018).

23. J. Liu, P. Wang, X. Zhang, Y. He, X. Zhou, H. Ye, Y. Li, S. Xu, S. Chen, and D. Fan, "Deep learning based atmospheric turbulence compensation for orbital angular momentum beam distortion and communication," Opt. Express **27**(12), 16671 (2019).